2014 5th IEEE RAS & EMBS International Conference on
Biomedical Robotics and Biomechatronics (BioRob)
August 12-15, 2014. São Paulo, Brazil

Variable Bipedal Walking Gait with Variable Leg Stiffness

Wesley Roozing, Ludo C. Visser, and Raffaella Carloni

Abstract— **The Spring-Loaded Inverted Pendulum (SLIP) model has been shown to exhibit many properties of human walking, and therefore has been the starting point for studies on robust, energy-efficient walking for robots. In this paper, the problem of gait variation during walking on the SLIP model is addressed by controlling the leg stiffness and the angle-of-attack in order to switch between gaits and thus regulate walking speeds. We show that it is possible to uniquely describe SLIP limit cycle gaits in fully normalised form. Using that description, we propose both an instantaneous switching method and an interpolation method with an optimisation step to switch between limit cycle SLIP gaits. Using simulations, we show that it is then possible to transition between them, after which the system converges back to zero-input limit cycle walking.**

I. INTRODUCTION

This work is inspired by the performance of human walking, which combines high robustness with high energy efficiency. In contrast, most existing legged robotic systems show either robustness or energy efficiency.

Passive dynamic walking can be realised by designing mechanics such that it has a walking gait as dynamic mode [1]. However, while designs based on the principle of passive dynamic walking show high energy efficiency, they are not very robust against external disturbances. Furthermore, these robots rely on compass gaits, using either stiff legs or locking the knee during walking, which does not resemble human legs. Other, highly controlled systems show high robustness at the exchange of energy efficiency [2]. Combining these two aspects has proven difficult.

It has been shown that human walking on flat terrain can be accurately modeled by an inverted passive mass-spring system. The Spring-Loaded Inverted Pendulum (SLIP) model shows walking dynamics strongly comparable to human walking in terms of hip trajectory, single- and double-support phases and ground contact forces [3]. It exhibits self-stable walking and running gait for a relatively large range of system parameters. It can demonstrate walking with different forward velocities as well as running [3], [4]. Although the SLIP model exhibits self-stable walking gait for large ranges of parameters on its own, it has been shown that the basin of attraction can be enlarged by control of a variable leg stiffness [5]. The Variable SLIP (V-SLIP) model significantly increases robustness against external disturbances and, after a disturbance, is able to restabilise the system into its original gait by injecting or removing energy appropriately.

It is desirable to be able to change the forward velocity of legged robots, for example slowing down to save energy, or speeding up to travel large distances quickly. In [7], it was shown that it is possible to change gait on the SLIP model by controlling the angle-of-attack. However, the method relies on imposing constant system energy, thus significantly reducing achievable velocities by injecting or removing energy in the system. In [8], the authors propose velocity control of a four-link walking model with stiff legs by changing step length and the frequency of the hip actuation. By placing their robot on a slope, they negate the loss of energy due to foot impacts and propose a velocity control strategy by controlling the slope. The work in [9] shows in simulation and experiment that it is possible to change velocity by changing step length and joint stiffnesses. They use variable stiffness actuators in each joint, but lock the stance leg knee to support the robot. A stiff-legged walker is used in [10], where the authors vary the pitch of a torso to induce different walking speeds. These works rely on compass gaits, using either stiff legs or locked knees during stance.

In this work, the problem of gait variation during walking is addressed by the design of a control strategy for the V-SLIP model that allows to switch between limit cycle gaits during walking by actively controlling the leg stiffness and angle-of-attack. We propose an optimisation criterion that aligns the two gaits and then switches between them by changing control references and system parameters appropriately, after which the system converges back to zero-input limit cycle walking. Energy is injected or removed from the system appropriately to accommodate the new gait.

The remainder of this paper is outlined as follows. Section II describes the SLIP model together with a normalised notation of SLIP limit cycle gaits. Section III outlines the strategy to control the V-SLIP system and switch between limit cycle gaits. Section V contains simulation results of the proposed method. Lastly, Section VI concludes on the work and proposes directions for future efforts.

Wesley Roozing is within the Department of Advanced Robotics, Istituto Italiano di Tecnologia, via Morego, 30, 16163 Genova. Email: wesley.roozing@iit.it (Research performed at the MIRA Institute, Faculty of Electrical Engineering, Mathematics, and Computer Science, University of Twente, The Netherlands). Raffaella Carloni is within the MIRA Institute, Faculty of Electrical Engineering, Mathematics, and Computer Science, University of Twente, The Netherlands. Email: r.carloni@utwente.nl

II. THE SPRING-LOADED INVERTED PENDULUM MODEL

A. SLIP Dynamics

The bipedal SLIP model is shown in Fig. 1. It consists of a hip point mass m, which connects two massless telescopic legs. The legs consist of springs with rest length L_0 and

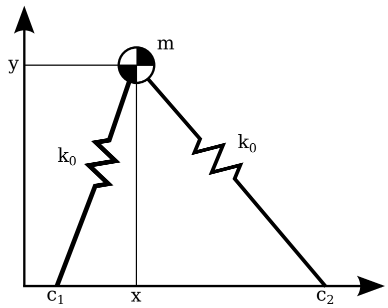

Fig. 1. The SLIP model consists of a hip point mass m, with two massless telescopic springs, with stiffnesses k_0, as legs. The model is shown during double-support phase, with both legs touching the ground at the foot contact points with x-positions c_1 and c_2.

stiffness k_0. Given properly chosen initial conditions, the SLIP model shows stable passive walking gaits [3], [4].

1) Configuration Manifold & State Transitions: The configuration of the system is given by the position of the hip mass as $(x, y) =: \mathbf{q} \in \mathcal{Q}$, and its velocity by $\dot{\mathbf{q}} \in T_{\mathbf{q}}\mathcal{Q}$, the tangent space to $\mathcal{Q}$ at $\mathbf{q}$. The system state is then given as $\mathbf{x} := (\mathbf{q}, \mathbf{p})$, with the momentum $\mathbf{p} := (p_x, p_y) = M\dot{\mathbf{q}}$ and the mass matrix $M = \mathrm{diag}(m, m)$. A single step is defined as a trajectory $\mathbf{q}(t) \in \mathcal{Q}$ that starts with the system in Vertical Leg Orientation (VLO), where the hip mass is exactly above the supporting leg and $c_1 = x$. The step ends when the system again reaches VLO (Fig. 2), and the role of the legs is then exchanged. We define the step length $L_g := x(T)$, i.e. the distance travelled after one step, where T is the gait time period.

During a single step, two phases must be distinguished – single-support (SS) and double-support (DS), during which one and two legs are in touch with the ground, respectively. The transition from single- to double-support occurs when the swing leg touches the ground, i.e. the mass reaches the touch-down height[1] y_{td} associated with the angle-of-attack α_0 and the rest length of the leg L_0 (Fig. 2):

$$y = y_{td} := L_0 \sin(\alpha_0) \tag{1}$$

The location of the leading foot contact position c_2 is then calculated as (Fig. 1):

$$c_2 = x + L_0 \cos(\alpha_0) \tag{2}$$

Similarly, the transition from double- to single-support occurs when either leg reaches its rest length[2]:

$$\sqrt{(x - c_i)^2 + y^2} = L_0\,, \quad i \in \{1, 2\} \tag{3}$$

At transition to single-support, the swing leg disappears and reappears at the subsequent instance of touch-down, which is possible because the leg is massless. In the nominal case, only the trailing leg reaches its rest length and contact c_2 is relabeled as c_1 to correspond to the notation used during

[1]Note that this implies that the hip height for SS is always higher than for DS.

[2]This ensures continuity of the system energy as there is no potential energy in the spring at lift-off.

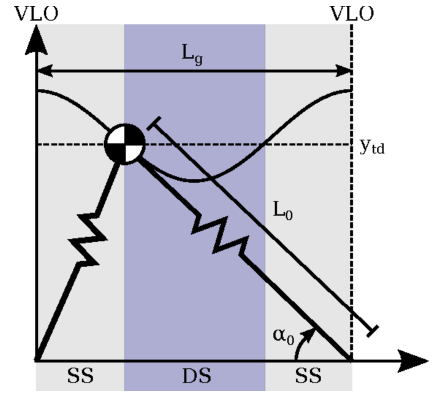

Fig. 2. A single step of the SLIP model, shown at the moment of touchdown. The step starts and ends at VLO and has length L_g. Note that at touchdown, the swing leg is at exactly α_0 with the ground and has length L_0. At touchdown, the SLIP model goes into double-support (DS) phase, shown by the touch-down height y_{td}, and returns into single-support (SS) phase when the trailing leg reaches length L_0 and the hip again crosses y_{td}.

single-support phase. We can now define two subsets of $\mathcal{Q}$ which correspond to the single- and double-support phases, respectively:

$$\begin{aligned} \mathcal{Q}_{SS} &= \{\mathbf{q} \in \mathcal{Q} \mid y > y_{td}\,,\ y < L_0\} \\ \mathcal{Q}_{DS} &= \{\mathbf{q} \in \mathcal{Q} \mid y < y_{td}\,,\ y > 0\} \end{aligned} \tag{4}$$

where $y < L_0$ and $y > 0$ are included to avoid the remaining cases, i.e. lift-off and fall respectively. Note that for a walking gait $\mathbf{q} \in \mathcal{Q}_{SS} \cup \mathcal{Q}_{DS}$. [3]

2) System Dynamics: To derive the dynamic equations for the system, we use the Hamiltonian approach. The kinetic energy function is defined as $K = \frac{1}{2}\mathbf{p}^T M^{-1}\mathbf{p}$ with $M := \mathrm{diag}(m, m)$ and the potential energy function as

$$V = mgy + \frac{1}{2}k_0 \left(L_0 - L_1\right)^2 + \frac{1}{2}k_0 \left(L_0 - L_2\right)^2$$

where $L_i = \sqrt{(x - c_i)^2 + y^2}$ and g is the gravitational acceleration. During single-support phase, we set $L_2 \equiv L_0$, i.e. the swing leg is uncompressed and it exerts no force. The dynamic equations are then defined by the Hamiltonian energy function $H = K + V$ as

$$\frac{\mathrm{d}}{\mathrm{d}t}\begin{bmatrix}\mathbf{q}\\ \mathbf{p}\end{bmatrix} = \begin{bmatrix}0 & I\\ -I & 0\end{bmatrix}\begin{bmatrix}\frac{\partial H}{\partial \mathbf{q}}\\ \frac{\partial H}{\partial \mathbf{p}}\end{bmatrix} \tag{5}$$

where I is the identity matrix. Note that a solution $\mathbf{q}(t)$ of (5) is of class C^2, due to the non-differentiability of the leg forces at the moment of transition between the single- and double-support phases.

B. Limit Cycle Gaits for the SLIP Model

It was shown in [4] that, given the proper system parameters and initial conditions, the dynamics described by (5) exhibit autonomous stable walking gait. A limit cycle gait

[3]Lift-off is also possible while $\mathbf{q} \in \mathcal{Q}_{SS} \cup \mathcal{Q}_{DS}$. We take care of this in simulation by checking $L_1 \leq L_0 \vee L_2 \leq L_0$, i.e. there is always at least one leg in contact with the ground.

is a periodic walking gait which returns to the same state periodically. From this point on, we refer to limit cycle gaits of the SLIP model as *natural gaits*.

In our description of natural gaits we use the state at VLO as initial conditions, i.e. $\mathbf{x}_0 = (\mathbf{q}, \mathbf{p})_0 = (x, y, p_x, p_y)_0$, and, during walking in natural gait, the system returns to this state at every VLO. Since we can take at VLO $x \equiv 0$, a natural gait Σ can then be fully described as

$$\Sigma = (\alpha_0, k_0, L_0, m, y_0, p_{x,0}, p_{y,0}) \tag{6}$$

Note that it is not possible to use the total system energy H to uniquely describe a natural gait, because energy can be stored in either potential or kinetic energy.

C. A Normalised Notation of SLIP Limit Cycle Gaits

k_0 and H can be normalised, such that SLIP models with different parameters can be compared easily:

$$\tilde{k} = k_0 \frac{L_0}{mg} \qquad \tilde{H} = \frac{H}{L_0 mg} \tag{7}$$

If we normalise $\mathbf{x}$ as $\tilde{\mathbf{x}} := (\tilde{\mathbf{q}}, \tilde{\mathbf{p}}) = (\tilde{x}, \tilde{y}, \tilde{p}_x, \tilde{p}_y)$ with

$$\tilde{x} = \frac{x}{L_0} \quad \tilde{y} = \frac{y}{L_0} \quad \tilde{p}_x = \frac{p_x}{m\sqrt{L_0 g}} \quad \tilde{p}_y = \frac{p_y}{m\sqrt{L_0 g}} \tag{8}$$

and use (7), we obtain a fully normalised unique description $\tilde{\Sigma}$ of a natural gait:

$$\tilde{\Sigma} = \left(\alpha_0, \tilde{k}, \tilde{y}_0, \tilde{p}_{x,0}, \tilde{p}_{y,0}\right) \tag{9}$$

The gait trajectory can then be found by solving (5) for $\tilde{\Sigma}$. Using this description, equal gaits on different SLIP systems now result in the same normalised state trajectory $\tilde{\mathbf{x}}(t) = (\tilde{\mathbf{q}}(t), \tilde{\mathbf{p}}(t))$. Similarly to $\tilde{p}_x, \tilde{p}_y$, the velocities are normalised as

$$\dot{\tilde{x}} = \frac{\dot{x}}{\sqrt{L_0 g}} \qquad \dot{\tilde{y}} = \frac{\dot{y}}{\sqrt{L_0 g}} \tag{10}$$

Note that the normalisation $\dot{\tilde{x}}$ is the Froude number Fr [9], [10], used to compare the relative walking speeds of systems with different leg lengths.

III. CONTROL DESIGN

By actively controlling the leg stiffness of the SLIP model, the robustness of the system to external disturbances can be significantly increased and, after a disturbance, the system can be stabilised into its original gait by injecting or removing energy appropriately [5]. The extended model, called V-SLIP, replaces the constant stiffness legs by variable stiffness legs.

We use the ability to change the leg stiffness to transition between gaits. The rationale is as follows. By considering a gait switch as a disturbance to the system which has to be rejected, the system can be controlled into any gait which is within the basin of attraction of the closed loop system. Furthermore, because there are large continuous regions of self-stable natural gaits with different forward velocities [4], the system can change into nearly any gait by using an appropriate transition strategy. In this section, we discuss the leg stiffness control that stabilises the system into a natural gait. The next section will discuss the gait transition strategy.

The variable stiffness legs of the V-SLIP model have stiffness $k_i = k_0 + u_i$, where k_i corresponds to the leg with contact c_i, and control inputs u_i restricted to subsets $U_i = \{u_i \in \mathbb{R} | 0 < k_0 + u_i < \infty\}$, such that the result is physically meaningful. Given a natural SLIP gait $\tilde{\Sigma}$ and corresponding state trajectory $\tilde{\mathbf{x}}(t)$, which is a solution of (5), we intend to control the system such that it converges to its natural gait, i.e. a reference $\tilde{\mathbf{x}}^{\circ}(t)$ such that $u_i \to 0$ and $k_i \to k_0$, $i \in \{1, 2\}$. However, as the system is underactuated during the single-support phase, these references cannot be tracked exactly, and as the system lags behind the reference this may lead to instability. Because $\tilde{x}$ was identified as a periodic variable, and required to be monotonically increasing in time, the references may be reparametrised in $\tilde{x}$. Due to the parametrisation in $\tilde{x}$, the gait references are sufficiently described as

$$\tilde{y}^*(\tilde{x}) = \tilde{y}^o(\tilde{x}) \qquad \dot{\tilde{x}}^*(\tilde{x}) = \dot{\tilde{x}}^o(\tilde{x}) \tag{11}$$

However, as a general analytic expression for the spring-loaded pendulum does not exist [11], a Fourier series expansion approximation of the numerical solution is used.

To formulate the control strategy, we rewrite Eq. (5) in standard form as

$$\dot{\mathbf{x}} = f(\mathbf{x}) + \sum_i g_i(\mathbf{x}) u_i \tag{12}$$

and then define error functions h_1 and h_2 as

$$\begin{aligned} h_1 &= y - y^* \\ h_2 &= \dot{x} - \dot{x}^* \end{aligned} \tag{13}$$

The control solution is then given as follows.

- For $\mathbf{q} \in \mathcal{Q}_{SS}$:

$$\begin{aligned} u_1 &= \frac{1}{\mathcal{L}_{g_1}\mathcal{L}_f h_1}\left(-\mathcal{L}_f^2 h_1 - \kappa_d \mathcal{L}_f h_1 - \kappa_p h_1\right) \\ u_2 &\equiv 0 \end{aligned} \tag{14}$$

- For $\mathbf{q} \in \mathcal{Q}_{DS}$:

$$\begin{bmatrix} u_1 \\ u_2 \end{bmatrix} = A^{-1} \begin{bmatrix} -\mathcal{L}_f^2 h_1 - \kappa_d \mathcal{L}_f h_1 - \kappa_p h_1 \\ -\mathcal{L}_f h_2 - \kappa_v h_2 \end{bmatrix} \tag{15}$$

  with

$$A = \begin{bmatrix} \mathcal{L}_{g_1}\mathcal{L}_f h_1 & \mathcal{L}_{g_2}\mathcal{L}_f h_1 \\ \mathcal{L}_{g_1}\mathcal{L}_f h_2 & \mathcal{L}_{g_2}\mathcal{L}_f h_2 \end{bmatrix} \tag{16}$$

where $\mathcal{L}_f^2 h_i$, $\mathcal{L}_f h_i$ and $\mathcal{L}_{g_i}\mathcal{L}_f h_i$ denote the (repeated) Lie-derivatives of h_i along the vector fields defined in (12) and $\kappa_d, \kappa_p, \kappa_v$ are tunable control parameters. The control inputs (14), (15) ensure that the error h_1 converges asymptotically to zero and that the error h_2 is at least bounded [5], [6].

Remark: Due to the structure of the problem, the system is not fully controllable during the single-support phase. Because the error in y influences touch-down and lift-off events, it is deemed more important. Thus, by design, only h_1 is controlled during the single-support phase (Eq. (14)).

Remark: During either single- or double-support, the control inputs u_1 and u_2 are continuous. However, their continuity is not guaranteed at the moment of phase transition.

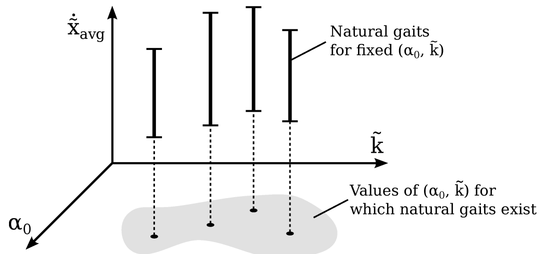

Fig. 3. Average forward velocities $\dot{\tilde{\mathbf{x}}}_{avg}$ of natural gaits for different values of $(\alpha_0, \tilde{k})$. Note that for given $(\alpha_0, \tilde{k})$, the average forward velocity is proportional to the system energy $\tilde{H}$.

IV. GAIT TRANSITION

A. Search of Stable Gaits

Suppose the system described by the SLIP model is in some natural gait and it is commanded to change the velocity. As natural gaits exist for large ranges of parameters, there often exists a range of natural gaits that achieve that velocity. This is shown in Fig. 3. Natural gaits exist for many values of $(\alpha_0, \tilde{k})$, and a single set $(\alpha_0, \tilde{k})$ can in general achieve a range of average forward velocities (vertical bar in Fig. 3).

Exactly which values of $(\alpha_0, \tilde{k})$ are chosen is arbitrary within the ranges of natural gaits. The next sections describe a general method for switching from some given gait $\tilde{\Sigma}_i$ to some other given gait $\tilde{\Sigma}_j$, independently of $\tilde{\Sigma}_i$ and $\tilde{\Sigma}_j$. We do, however, make a distinction between switching between gaits with equal values of $(\alpha_0, \tilde{k})$ (Section IV-C.1) and gaits with different $(\alpha_0, \tilde{k})$ (Section IV-C.2).

B. Optimisation Criterion for Gait Switching

1) Finding Optimal Points: Suppose that two natural gaits $\tilde{\Sigma}_i$ and $\tilde{\Sigma}_j$ have been chosen and that we want the system to switch from $\tilde{\Sigma}_i$ to $\tilde{\Sigma}_j$. The parametrisation in $\tilde{x}$ of both can be used to determine exactly how to transition from one gait to the other. In each gait one point should be considered: the point in $\tilde{\Sigma}_i$ at which the switch is executed and the point in $\tilde{\Sigma}_j$ to switch into. Fig. 4 shows example trajectories of $\tilde{\Sigma}_i$ and $\tilde{\Sigma}_j$. Any point $\tilde{x}_i \in [0, \tilde{L}_{g,i}]$ on one step of $\tilde{\Sigma}_i$ can be associated with any point $\tilde{x}_j \in [0, \tilde{L}_{g,j}]$ on one step of $\tilde{\Sigma}_j$. A combination of two values $(\tilde{x}_{i,opt}, \tilde{x}_{j,opt})$ should exist that minimises some criterion J. Intuitively, to minimise the required control input for transition, we propose to transition at a point at which both gaits have approximately equal momentum of the hip mass, that is, $\mathbf{p}_i(x_i) \approx \mathbf{p}_j(x_j)$ (Fig. 4). However, as m is constant, the velocities $\left(\dot{\tilde{x}}, \dot{\tilde{y}}\right)$ are used. As the forward velocity is only controlled during double-support phase, whereas the vertical position is controlled during both single- and double-support, differences in $\dot{\tilde{x}}$ are penalised differently than in $\dot{\tilde{y}}$. Thus, both terms are included separately. Additionally, we include the hip height $\tilde{y}$, as it would be beneficial to switch at a point at which the trajectories are close together, such that the resulting error

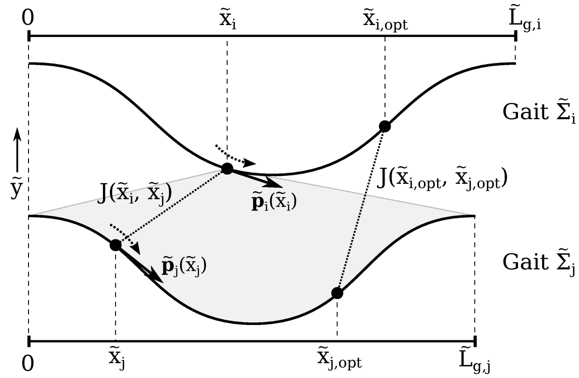

Fig. 4. Optimisation of the switching point from $\tilde{\Sigma}_i$ to $\tilde{\Sigma}_j$. The point $\tilde{x}_i$ is moved along one step of $\tilde{\Sigma}_i$, and $J(\tilde{x}_i, \tilde{x}_j)$ is then calculated for all values of $\tilde{x}_j$ in one step of $\tilde{\Sigma}_j$. Minimisation of J for both these parameters then results in the optimal switching points $(\tilde{x}_{i,opt}, \tilde{x}_{j,opt})$. Note that the gaits shown here are far apart in $\tilde{y}$, while in practice many gaits will partially overlap, especially those with equal values of α_0.

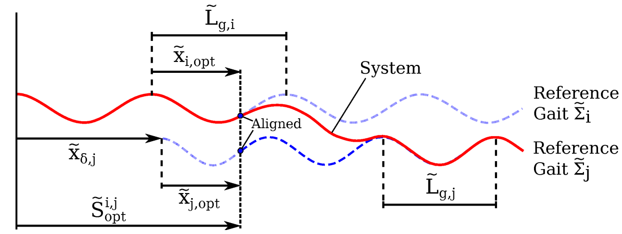

Fig. 5. Aligning optimal points of $\tilde{\Sigma}_i$ and $\tilde{\Sigma}_j$, with step lengths $\tilde{L}_{g,i}$ and $\tilde{L}_{g,j}$, respectively. The trajectory of $\tilde{\Sigma}_j$ is shifted by $\tilde{x}_{\delta,j}$, such that $\tilde{x}_{j,opt}$ aligns with $\tilde{x}_{i,opt}$ at the optimal switching distance $\tilde{S}^{i,j}_{opt}$. The dashed blue lines indicate the natural gait references, the red line indicates an example gait transition.

h_1 is smaller. We then define $J(\tilde{x}_i, \tilde{x}_j)$ as follows:

$$\begin{aligned} J(\tilde{x}_i, \tilde{x}_j) = \mu_1 \left\|\tilde{y}_j(\tilde{x}_j) - \tilde{y}_i(\tilde{x}_i)\right\| + \\ \mu_2 \left\|\dot{\tilde{x}}_j(\tilde{x}_j) - \dot{\tilde{x}}_i(\tilde{x}_i)\right\| + \\ \mu_3 \left\|\dot{\tilde{y}}_j(\tilde{x}_j) - \dot{\tilde{y}}_i(\tilde{x}_i)\right\| \end{aligned} \tag{17}$$

By choosing the weights $\mu_{1,2,3}$, the different aspects of the gait can be emphasised as to achieve a smooth response. The criterion J is then minimised numerically with respect to $\tilde{x}_i$ and $\tilde{x}_j$ to obtain the optimal switching points:

$$\min_{\tilde{x}_i, \tilde{x}_j} J(\tilde{x}_i, \tilde{x}_j) \rightarrow (\tilde{x}_{i,opt}, \tilde{x}_{j,opt}) \tag{18}$$

Note that multiple minima may exist, so we search for the global minimum. Due to the use of normalised variables the results are again identical for the same natural gaits on different SLIP systems, and due to symmetry results obtained for the switch $\tilde{\Sigma}_i \rightarrow \tilde{\Sigma}_j$ are also valid for $\tilde{\Sigma}_j \rightarrow \tilde{\Sigma}_i$.

2) Aligning optimal points: As gaits are parametrised as a function of forward distance $\tilde{x}$, we define the gait transitions in terms of forward distance as well. The switching strategy for a single transition is then summarized as follows. Suppose the system is commanded to switch into gait $\tilde{\Sigma}_j$ at a distance $S^{i,j}_{com}$ [m], normalised as $\tilde{S}^{i,j}_{com} = S^{i,j}_{com}/L_0$. We then calculate the optimal switching distance $\tilde{S}^{i,j}_{opt}$, which is the first occurrence of the point $\tilde{x}_{i,opt}$ after this commanded

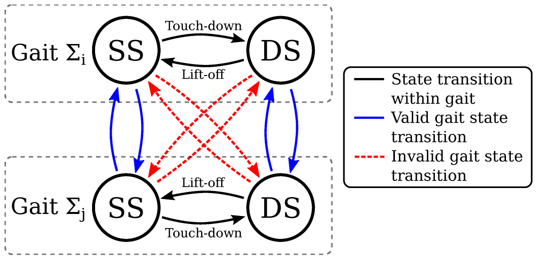

Fig. 6. State transitions during limit cycle walking and gait transition. For a single gait, a transition from single-support to double-support and back occurs every step. When switching gaits in single-support, the system transitions to single-support of the new gait, and vice versa. A transition from double-support of gait $\tilde{\Sigma}_i$ to single-support of gait $\tilde{\Sigma}_j$ (or vice versa) is invalid, as that would require foot lift-off at the moment the controller decides to switch gaits, which is infeasible.

distance (Fig. 5):

$$\tilde{S}^{i,j}_{opt} = \tilde{S}^{i,j}_{com} - \tilde{S}^{i,j}_{com}(\mathrm{mod}\tilde{L}_{g,i}) + \tilde{x}_{i,opt} \tag{19}$$

If $\tilde{S}^{i,j}_{opt} < \tilde{S}^{i,j}_{com}$, we make sure the switching distance is after the commanded distance by calculating $\tilde{S}^{i,j}_{opt} = \tilde{S}^{i,j}_{opt} + \tilde{L}_{g,i}$, that is, delaying the switch by exactly one step. Once the optimal point in the current gait has been reached, the system can switch into the new gait by changing α_0, $\tilde{k}$, and the controller references appropriately.

To ensure the system switches from the optimal point in the step of $\tilde{\Sigma}_i$ into the optimal point in the step of $\tilde{\Sigma}_j$, the trajectory of $\tilde{\Sigma}_j$ is shifted in such a way that the point $\tilde{x}_{j,opt}$ aligns with $\tilde{S}^{i,j}_{opt}$ in $\tilde{x}$. The shift $\tilde{x}_{\delta,j}$ of $\tilde{\Sigma}_j$ is calculated as

$$\tilde{x}_{\delta,j} = \tilde{S}^{i,j}_{opt} - \tilde{x}_{j,opt} \tag{20}$$

By shifting the reference of $\tilde{\Sigma}_j$ by $\tilde{x}_{\delta,j}$, the optimal points $(\tilde{x}_{i,opt}, \tilde{x}_{j,opt})$ are aligned in $\tilde{x}$ (Fig. 5). The calculations described in this section are not computationally intensive, allowing them to be done on-line.

C. Switching Strategy

In this section we outline the switching strategy. Although the method is general, we make a distinction between switching between gaits with equal values of $(\alpha_0, \tilde{k})$ and gaits with different $(\alpha_0, \tilde{k})$. The first case will be shown to be a particular case of the second.

Fig. 6 shows the possible states and transitions for some gaits $\tilde{\Sigma}_i$ and $\tilde{\Sigma}_j$. For a single gait, a transition from single-support to double-support and back occurs every step, at touch-down and lift-off respectively (i.e. when $\tilde{y}$ crosses $\tilde{y}_{td}$). However, if the two gaits have different values of α_0, the current hip height may be defined as double-support in $\tilde{\Sigma}_i$, but as single-support in $\tilde{\Sigma}_j$, i.e. $\tilde{y}_{td,i} > \tilde{y} > \tilde{y}_{td,j}$. This results in an invalid situation if the gait switching is performed instantaneous at that point, as that would require instantaneous foot lift-off at the instant of switching.

However, we do not want to rule out such points entirely by modification of (17). Firstly, because at such points the gait trajectories may be close together in terms of hip height $\tilde{y}$ resulting in smaller error h_1. Secondly, large variations in α_0 may cause gaits to be entirely separated in $\tilde{y}$, such as in Fig. 4, where the entire gait $\tilde{\Sigma}_j$ lies under the touch-down height of $\tilde{\Sigma}_i$. Therefore, for gaits with equal values of $(\alpha_0, \tilde{k})$ instantaneous switching is used, and for gaits with different $(\alpha_0, \tilde{k})$ gait interpolation is used, as outlined below.

1) Instantaneous Switching: As the values of $(\alpha_0, \tilde{k})$ remain constant, we need only to define the controller references $\left(\tilde{y}^*(\tilde{x}), \dot{\tilde{x}}^*(\tilde{x})\right)$ as:

$$\begin{aligned}
\tilde{y}^*(\tilde{x}) &= \begin{cases} \tilde{y}^o_i(\tilde{x}) & \tilde{x} < \tilde{S}^{i,j}_{opt} \\ \tilde{y}^o_j(\tilde{x} - \tilde{x}_{\delta,j}) & \tilde{x} \geq \tilde{S}^{i,j}_{opt} \end{cases} \\
\dot{\tilde{x}}^*(\tilde{x}) &= \begin{cases} \dot{\tilde{x}}^o_i(\tilde{x}) & \tilde{x} < \tilde{S}^{i,j}_{opt} \\ \dot{\tilde{x}}^o_j(\tilde{x} - \tilde{x}_{\delta,j}) & \tilde{x} \geq \tilde{S}^{i,j}_{opt} \end{cases}
\end{aligned} \tag{21}$$

2) Gait Interpolation: To avoid invalid gait transitions (Fig. 6) caused by instantaneously changing the value of α_0, we need to ensure the value of α_0 is continuous in $\tilde{x}$. This way we avoid the invalid state transitions in Fig. 6. We extend (21) with a transition period, during which the two gait references are interpolated, together with the corresponding values of α_0 and $\tilde{k}$:

$$\begin{aligned}
\tilde{y}^*(\tilde{x}) &= \begin{cases} \tilde{y}^o_i(\tilde{x}) & \beta \leq 0 \\ (1-\beta)\tilde{y}^o_i(\tilde{x}) + \beta\tilde{y}^o_j(\tilde{x} - \tilde{x}_{\delta,j}) & 0 < \beta < 1 \\ \tilde{y}^o_j(\tilde{x} - \tilde{x}_{\delta,j}) & \beta \geq 1 \end{cases} \\
\dot{\tilde{x}}^*(\tilde{x}) &= \begin{cases} \dot{\tilde{x}}^o_i(\tilde{x}) & \beta \leq 0 \\ (1-\beta)\dot{\tilde{x}}^o_i(\tilde{x}) + \beta\dot{\tilde{x}}^o_j(\tilde{x} - \tilde{x}_{\delta,j}) & 0 < \beta < 1 \\ \dot{\tilde{x}}^o_j(\tilde{x}) & \beta \geq 1 \end{cases} \\
\alpha_0 &= \begin{cases} \alpha_{0,i} & \beta \leq 0 \\ (1-\beta)\alpha_{0,i} + \beta\alpha_{0,j} & 0 < \beta < 1 \\ \alpha_{0,j} & \beta \geq 1 \end{cases} \\
\tilde{k} &= \begin{cases} \tilde{k}_i & \beta \leq 0 \\ (1-\beta)\tilde{k}_i + \beta\tilde{k}_j & 0 < \beta < 1 \\ \tilde{k}_j & \beta \geq 1 \end{cases}
\end{aligned} \tag{22}$$

where the interpolation factor β is defined as $\beta = (\tilde{x} - \tilde{S}^{i,j}_{opt})/\gamma$. The parameter $\gamma \geq 0$ is the transition length. By the definition of the normalised variables, γ effectively is the number of leg lengths in x to interpolate for. Of course, $\left(\tilde{y}^*, \dot{\tilde{x}}^*\right)$ in (22) converge to (21) as $\gamma \to 0$. The reason we use (21) for constant $(\alpha_0, \tilde{k})$ is that then we let the controller handle the transition as quick as possible, instead of forcing a transition period of fixed length.

V. RESULTS

To demonstrate the effectiveness of the method for large forward velocity differences, first achievable velocity ranges for selected values of $(\alpha_0, \tilde{k})$ that result in symmetric natural gaits is analysed. Simulations were performed in Mathworks MATLAB R2012b, using the ode45 solver with absolute and relative tolerances of 1e-10. The velocity ranges were found by fixing the vertical velocity at VLO to zero, thus enforcing symmetrical gaits [4], and incrementing the forward velocity at VLO in small steps. The resulting velocity ranges are shown in Table I, where $\dot{\tilde{x}}_{avg}$ denotes the normalised average forward velocity and $\dot{x}_{avg}$ denotes the average forward velocity in [m s^{-1}].

TABLE I

STABLE FORWARD VELOCITY RANGES FOR SYMMETRICAL GAITS WITH SELECTED VALUES OF $(\alpha_0, \tilde{k})$.

$(\alpha_0, \tilde{k})$	$\dot{\tilde{x}}_{avg}$ []	$\dot{x}_{avg}$ [m s^{-1}]
$(60, 8)$	0.239–0.344	0.750–1.079
$(62, 10)$	0.236–0.364	0.739–1.140
$(64, 11)$	0.229–0.361	0.719–1.132
$(66, 14)$	0.233–0.379	0.730–1.187
$(68, 16)$	0.229–0.378	0.718–1.183
$(70, 20)$	0.219–0.387	0.687–1.211
$(72, 23)$	0.226–0.380	0.706–1.189

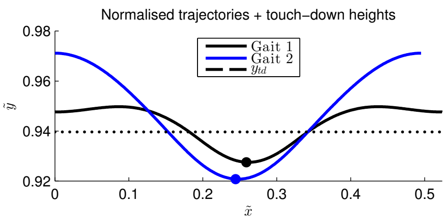

Fig. 7. Hip trajectories for a single step of two gaits with $(\alpha_0, \tilde{k}) = (70, 20)$. The slow gait (1) is double-humped, whereas the faster gait (2) is single-humped. The dotted line y_{td} denotes the touch-down height, and the solid dots denote the optimal points $(\tilde{x}_{1,opt}, \tilde{x}_{2,opt})$.

Two simulations are performed. In both cases, $m = 80$ kg and $L_0 = 1$ m. Furthermore, $\{\mu_1, \mu_2, \mu_3\} = \{15, 2, 5\}$. In the first simulation (Section V-A), a constant value $(\alpha_0, \tilde{k}) = (70, 20)$ is chosen, and two gaits are selected: a slow gait with average velocity of 0.238 (0.745 m s^{-1}, using (8)) and a fast gait with average velocity 0.372 (1.164 m s^{-1}), an increase of $\approx 56\%$. Switching between these two gaits corresponds to moving up and down on one of the vertical bars in Fig. 3, and we use the instantaneous switching method (Section IV-C.1).

In the second (Section V-B), a slow gait with an average velocity of 0.232 (0.725 m s^{-1}) and $(\alpha_0, \tilde{k}) = (64, 11)$ and a fast gait with an average velocity of 0.372 (1.164 m s^{-1}) and $(\alpha_0, \tilde{k}) = (70, 20)$ are chosen, to demonstrate the ability to change the angle of attack. In Fig. 3, this corresponds to switching from one point on a vertical bar to another point on another bar. Here we use the gait interpolation with $\gamma = 1.0$ (Section IV-C.2).

In both cases, the system starts in the slow gait (gait 1), commanded to change to fast gait (gait 2) at 1.0 m, and then switch back to the slow gait (gait 3 = gait 1) at 5.5 m.

A. Constant $(\alpha_0, \tilde{k})$

Fig. 7 shows the hip trajectory for a single step of both gaits. The first, i.e. slow gait, is double-humped, whereas the faster gait is single-humped. This likely results from the fact that the natural frequency of the hip mass and leg springs remains approximately constant, while the gait period changes. Calculating J for these two gaits results in $(\tilde{x}_{1,opt}, \tilde{x}_{2,opt}) = (0.259, 0.244)$, which corresponds almost to the lowest point in both gaits. Of course, for the switch back to the first gait we can use the same values but interchanged. The found values result in optimal switching distances $\tilde{S}^{1,2}_{opt} = 1.306$ and $\tilde{S}^{2,3}_{opt} = 5.762$ respectively (Eq. (19)).

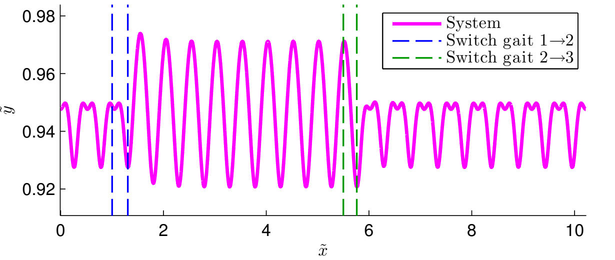

Fig. 8. Hip trajectory for the transition from slow to fast gait and back for two gaits with constant $(\alpha_0, \tilde{k})$. For each pair of vertical dashed lines, the first indicates the commanded switching distance, and the second indicates the resulting optimal switching distance.

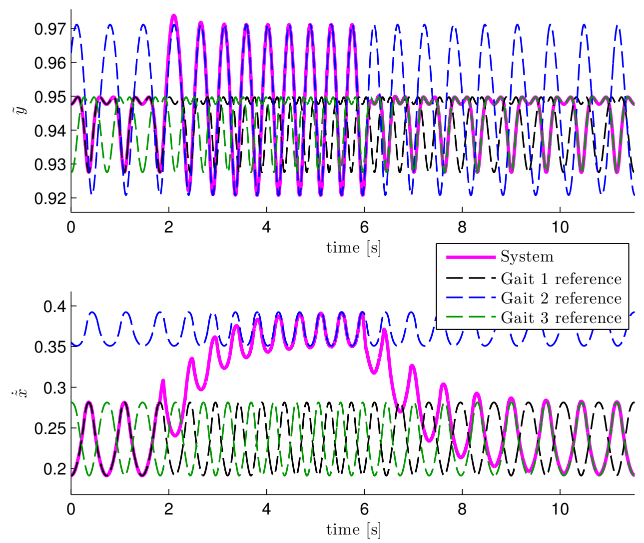

Fig. 9. Hip height and forward velocity over time. The vertical hip motion converges to the new reference within one step. The forward velocity converges in approximately 5 steps.

Fig. 8 shows the resulting hip trajectory with the desired and optimal switching points indicated. The hip returns to a periodic trajectory very quickly. Fig. 9 shows the resulting hip height and forward velocity in time, as well as the natural gait references. It can be seen that because the hip height is controlled during both single- and double-support, $\tilde{y}$ converges to the new reference within a single step. The forward velocity $\dot{\tilde{x}}$ converges to the new reference within approximately 5 steps in both transitions. Fig. 10 shows the control inputs and position and velocity errors. The disturbance that arises from the new references is rejected in approximately one second for the hip height and four seconds for the forward velocity respectively, after which the leg stiffnesses converge back to the nominal value. Fig. 11 shows the energy balance. The energy increases from $\tilde{H}_1 = 0.993$ to $\tilde{H}_2 = 1.041$ after the first switch, which if all converted to forward kinetic energy would result in a forward velocity of $\dot{\tilde{x}}_{avg} = 0.388$ (1.216 m s^{-1}). This shows that not all added energy is converted into forward momentum but

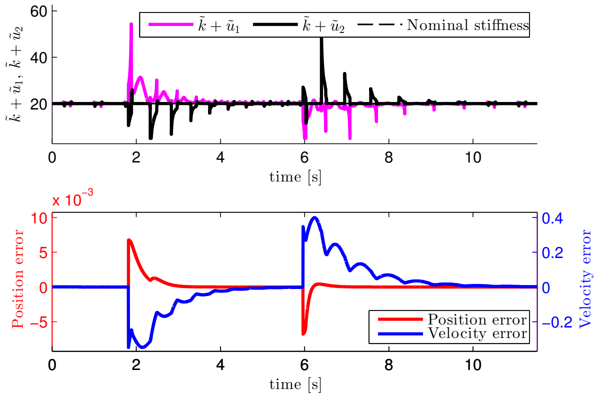

Fig. 10. Control input and error functions. The disturbances that arise from the new references are rejected, after which the leg stiffnesses converge back to their nominal values.

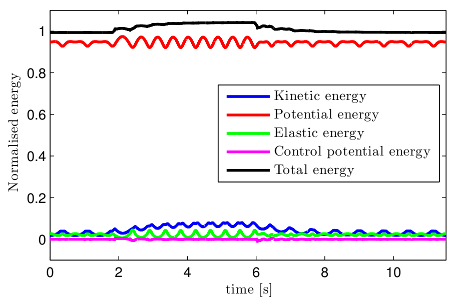

Fig. 11. Energy balance. Most of the increase in total energy is used in the kinetic energy of the system. Some of the additional energy results in increased vertical motion of the hip.

instead into vertical motion (Fig. 7) and a minor increase in average hip height.

Remark: The small periodic deviations in the inputs (Fig. 10) after convergence arise due to difference between the approximated gait references using Fourier series and the SLIP model dynamics.

B. Gaits with different $(\alpha_0, \tilde{k})$

Fig. 12 shows the hip trajectory for a single step of both gaits. It can be seen that due to the different values of α_0 the gaits are completely separated in hip height during the entire step; this also results in a significantly smaller step length for gait 2. Again calculating J for these two gaits,

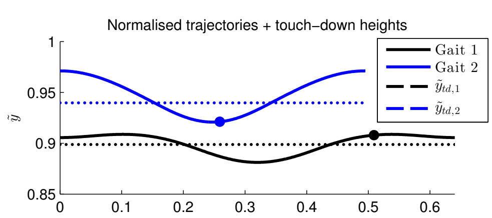

Fig. 12. Hip trajectories for a single step of two gaits with $(\alpha_0, \tilde{k}) = (64, 11)$ and $(70, 20)$ respectively. In contrast with Fig. 7, the gaits are completely separated in $\tilde{y}$ and have different touch-down heights $y_{td,i}$. The solid dots denote the optimal points $(\tilde{x}_{1,opt}, \tilde{x}_{2,opt})$.

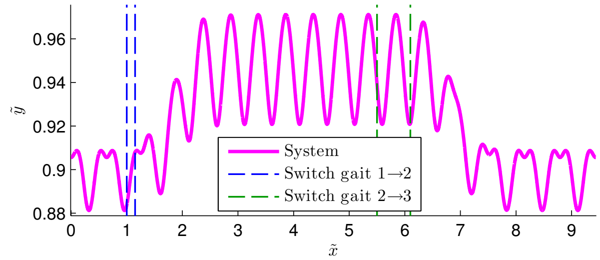

Fig. 13. Hip trajectory for the transition from slow to fast gait and back for two gaits with different $(\alpha_0, \tilde{k})$. For each pair of vertical dashed lines, the first indicates the commanded switching distance, and the second indicates the resulting optimal switching distance.

we find $(\tilde{x}_{1,opt}, \tilde{x}_{2,opt}) = (0.509, 0.259)$. This corresponds to approximately the highest point in the first gait and the lowest point in the second gait, arising from the separation of both gaits in terms of hip height. The found values result in optimal switching distances $\tilde{S}^{1,2}_{opt} = 1.090$ and $\tilde{S}^{2,3}_{opt} = 6.041$ respectively.

Fig. 13 shows the resulting hip trajectory with the desired and optimal switching points indicated. The trajectory smoothly rises to the new hip height as its shape transforms into that of the second gait. Inspecting the hip height and forward velocity over time (Fig. 14), we see a similar smooth transition. The hip oscillation frequency increases as α_0 and forward velocity increase. Note how the forward velocity suddenly increases as the system transitions back to the first gait. This is due to α_0 decreasing, thus lowering touch-down height, leaving more time for the hip mass to accelerate before touch-down. Fig. 15 shows the corresponding control input and error functions. On a few occasions, the leg stiffness reaches the lower limit. After transition, the leg stiffnesses converge to the new gait's nominal $\tilde{k}$ value. Note that during single-support, the stiffness of the swing leg is always equal to $\tilde{k}$ (Eq. (22)), as $\tilde{u}_2 \equiv 0$ in that case (Eq. (14)). The total energy again increases to accommodate the faster gait. The increase is converted in both kinetic and potential energy, while the average elastic energy decreases. The latter can be attributed to the higher, more stiff-legged walk of the second gait.

VI. CONCLUSIONS & FUTURE WORK

A method was presented that allows a bipedal V-SLIP model to switch between natural gaits by actively controlling the leg stiffness. Using this method it is possible to vary the forward velocity during walking by choosing appropriate natural gaits.

First, a normalised notation of natural gaits was introduced. Next a optimisation step was proposed that aligns two chosen gaits by minimisation of a criterion, designed such that the transition between the two is as smooth as possible. The switch was performed in one of two possible ways; instantaneous switching for gaits with equal values of the angle of attack and leg stiffness, and gait interpolation with gaits with different values.

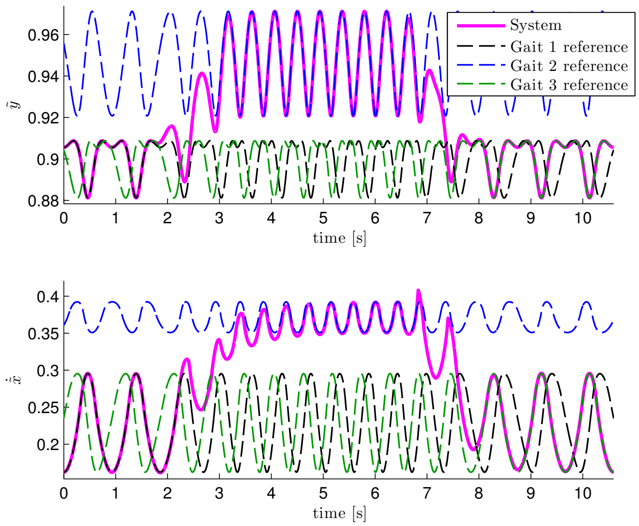

Fig. 14. Hip height and forward velocity over time. The vertical hip motion and forward velocity converge to the new gait in approximately 3 steps.

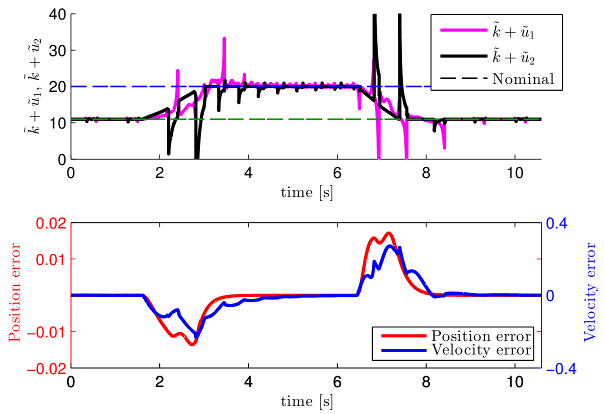

Fig. 15. Control input and error functions. The disturbances that arise from the new references are rejected, after which the leg stiffness converges to a constant value. Note that during single-support, the stiffness of the swing leg is always equal to $\tilde{k}$, as $\tilde{u}_2 \equiv 0$ in that case (Eq. (14)).

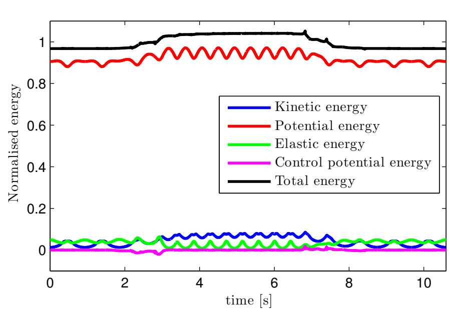

Fig. 16. Energy balance. In the first gait, there is relatively much energy stored as elastic energy, due to the lower leg stiffness. Compared to Fig. 11, there is a significant rise in the potential energy due to the increased hip height of the second gait.

It was shown that in both cases the system can be controlled from gait to gait within approximately 5 steps. In both cases, the hip trajectory converges within two steps, but the forward velocity takes longer to converge. After the transition, control action converges to zero as the system converges into limit cycle walking.

Future work should focus on analysing the robustness of the system during gait transition. Furthermore, it could include a study on more realistic models, such as those including knees and feet, or non-zero leg mass.

References

[1] T. McGeer, "Passive dynamic walking," *The International Journal of Robotics Research*, vol. 9, no. 2, pp. 62–82, 1990.

[2] S. Collins and A. Ruina, "A bipedal walking robot with efficient and human-like gait," *IEEE International Conference on Robotics and Automation*, 2005.

[3] H. Geyer, A. Seyfarth, and R. Blickhan, "Compliant leg behaviour explains basic dynamics of walking and running," in *The Royal Society B, Biological Sciences*, vol. 273, no. 1603, pp. 2861–7, 2006.

[4] J. Rummel, Y. Blum, and A. Seyfarth, "Robust and efficient walking with spring-like legs," *Bioinspiration and Biomimetics*, vol. 5, no. 4, p. 16, 2010.

[5] L. C. Visser, S. Stramigioli, and R. Carloni, "Robust Bipedal Walking with Variable Leg Stiffness," in *IEEE RAS/EMBS International Conference on Biomedical Robotics and Biomechatronics*, pp. 1626–1631, 2012.

[6] A. Isidori, *Nonlinear Control Systems*, 3rd ed., 1995.

[7] H. R. Martinez Salazar and J. P. Carbajal, "Exploiting the passive dynamics of a compliant leg to develop gait transitions," *Physical Review E*, vol. 83, no. 6, p. 066707, 2011.

[8] T. Haarnoja, J.-L. Peralta-Cabezas, and A. Halme, "Model-based velocity control for Limit Cycle Walking," *IEEE/RSJ International Conference on Intelligent Robots and Systems*, pp. 2255–2260, 2011.

[9] Y. Huang, B. Vanderborght, R. Van Ham, Q. Wang, M. Van Damme, G. Xie, and D. Lefeber, "Step Length and Velocity Control of a Dynamic Bipedal Walking Robot With Adaptable Compliant Joints," *IEEE/ASME Transactions on Mechatronics*, vol. 18, no. 2, pp. 598–611, 2013.

[10] D. G. E. Hobbelen and M. Wisse, "Controlling the Walking Speed in Limit Cycle Walking," *The International Journal of Robotics Research*, vol. 27, no. 9, pp. 989–1005, 2008.

[11] S. V. Kuznetsov, "The motion of the elastic pendulum," *Regular and Chaotic Dynamics*, vol. 4, no. 3, pp. 3–12, 1999.